First Observation of the Decay $B_s^0 \to D_s^- D_s^+$ and Measurement of Its Branching Ratio

T. Aaltonen,[23] J. Adelman,[13] T. Akimoto,[54] M. G. Albrow,[17] B. Álvarez González,[11] S. Amerio,[42] D. Amidei,[34] A. Anastassov,[51] A. Annovi,[19] J. Antos,[14] M. Aoki,[24] G. Apollinari,[17] A. Apresyan,[47] T. Arisawa,[56] A. Artikov,[15] W. Ashmanskas,[17] A. Attal,[3] A. Aurisano,[52] F. Azfar,[41] P. Azzi-Bacchetta,[42] P. Azzurri,[45] N. Bacchetta,[42] W. Badgett,[17] A. Barbaro-Galtieri,[28] V. E. Barnes,[47] B. A. Barnett,[25] S. Baroiant,[7] V. Bartsch,[30] G. Bauer,[32] P.-H. Beauchemin,[33] F. Bedeschi,[45] P. Bednar,[14] S. Behari,[25] G. Bellettini,[45] J. Bellinger,[58] A. Belloni,[22] D. Benjamin,[16] A. Beretvas,[17] J. Beringer,[28] T. Berry,[29] A. Bhatti,[49] M. Binkley,[17] D. Bisello,[42] I. Bizjak,[30] R. E. Blair,[2] C. Blocker,[6] B. Blumenfeld,[25] A. Bocci,[16] A. Bodek,[48] V. Boisvert,[48] G. Bolla,[47] A. Bolshov,[32] D. Bortoletto,[47] J. Boudreau,[46] A. Boveia,[10] B. Brau,[10] A. Bridgeman,[24] L. Brigliadori,[5] C. Bromberg,[35] E. Brubaker,[13] J. Budagov,[15] H. S. Budd,[48] S. Budd,[24] K. Burkett,[17] G. Busetto,[42] P. Bussey,[21] A. Buzatu,[33] K. L. Byrum,[2] S. Cabrera,[16,s] M. Campanelli,[35] M. Campbell,[34] F. Canelli,[17] A. Canepa,[44] D. Carlsmith,[58] R. Carosi,[45] S. Carrillo,[18,m] S. Carron,[33] B. Casal,[11] M. Casarsa,[17] A. Castro,[5] P. Catastini,[45] D. Cauz,[53] M. Cavalli-Sforza,[3] A. Cerri,[28] L. Cerrito,[30,q] S. H. Chang,[27] Y. C. Chen,[1] M. Chertok,[7] G. Chiarelli,[45] G. Chlachidze,[17] F. Chlebana,[17] K. Cho,[27] D. Chokheli,[15] J. P. Chou,[22] G. Choudalakis,[32] S. H. Chuang,[51] K. Chung,[12] W. H. Chung,[58] Y. S. Chung,[48] C. I. Ciobanu,[24] M. A. Ciocci,[45] A. Clark,[20] D. Clark,[6] G. Compostella,[42] M. E. Convery,[17] J. Conway,[7] B. Cooper,[30] K. Copic,[34] M. Cordelli,[19] G. Cortiana,[42] F. Crescioli,[45] C. Cuenca Almenar,[7,s] J. Cuevas,[11,p] R. Culbertson,[17] J. C. Cully,[34] D. Dagenhart,[17] M. Datta,[17] T. Davies,[21] P. de Barbaro,[48] S. De Cecco,[50] A. Deisher,[28] G. De Lentdecker,[48,e] G. De Lorenzo,[3] M. Dell'Orso,[45] L. Demortier,[49] J. Deng,[16] M. Deninno,[5] D. De Pedis,[50] P. F. Derwent,[17] G. P. Di Giovanni,[43] C. Dionisi,[50] B. Di Ruzza,[53] J. R. Dittmann,[4] M. D'Onofrio,[3] S. Donati,[45] P. Dong,[8] J. Donini,[42] T. Dorigo,[42] S. Dube,[51] J. Efron,[38] R. Erbacher,[7] D. Errede,[24] S. Errede,[24] R. Eusebi,[17] H. C. Fang,[28] S. Farrington,[29] W. T. Fedorko,[13] R. G. Feild,[59] M. Feindt,[26] J. P. Fernandez,[31] C. Ferrazza,[45] R. Field,[18] G. Flanagan,[47] R. Forrest,[7] S. Forrester,[7] M. Franklin,[22] J. C. Freeman,[28] I. Furic,[18] M. Gallinaro,[49] J. Galyardt,[12] F. Garberson,[10] J. E. Garcia,[45] A. F. Garfinkel,[47] H. Gerberich,[24] D. Gerdes,[34] S. Giagu,[50] V. Giakoumopolou,[45,b] P. Giannetti,[45] K. Gibson,[46] J. L. Gimmell,[48] C. M. Ginsburg,[17] N. Giokaris,[15,b] M. Giordani,[53] P. Giromini,[19] M. Giunta,[45] V. Glagolev,[15] D. Glenzinski,[17] M. Gold,[36] N. Goldschmidt,[18] A. Golossanov,[17] G. Gomez,[11] G. Gomez-Ceballos,[32] M. Goncharov,[52] O. González,[31] I. Gorelov,[36] A. T. Goshaw,[16] K. Goulianos,[49] A. Gresele,[42] S. Grinstein,[22] C. Grosso-Pilcher,[13] R. C. Group,[17] U. Grundler,[24] J. Guimaraes da Costa,[22] Z. Gunay-Unalan,[35] C. Haber,[28] K. Hahn,[32] S. R. Hahn,[17] E. Halkiadakis,[51] A. Hamilton,[20] B.-Y. Han,[48] J. Y. Han,[48] R. Handler,[58] F. Happacher,[19] K. Hara,[54] D. Hare,[51] M. Hare,[55] S. Harper,[41] R. F. Harr,[57] R. M. Harris,[17] M. Hartz,[46] K. Hatakeyama,[49] J. Hauser,[8] C. Hays,[41] M. Heck,[26] A. Heijboer,[44] B. Heinemann,[28] J. Heinrich,[44] C. Henderson,[32] M. Herndon,[58] J. Heuser,[26] S. Hewamanage,[4] D. Hidas,[16] C. S. Hill,[10,d] D. Hirschbuehl,[26] A. Hocker,[17] S. Hou,[1] M. Houlden,[29] S.-C. Hsu,[9] B. T. Huffman,[41] R. E. Hughes,[38] U. Husemann,[59] J. Huston,[35] J. Incandela,[10] G. Introzzi,[45] M. Iori,[50] A. Ivanov,[7] B. Iyutin,[32] E. James,[17] B. Jayatilaka,[16] D. Jeans,[50] E. J. Jeon,[27] S. Jindariani,[18] W. Johnson,[7] M. Jones,[47] K. K. Joo,[27] S. Y. Jun,[12] J. E. Jung,[27] T. R. Junk,[24] T. Kamon,[52] D. Kar,[18] P. E. Karchin,[57] Y. Kato,[40] R. Kephart,[17] U. Kerzel,[26] V. Khotilovich,[52] B. Kilminster,[38] D. H. Kim,[27] H. S. Kim,[27] J. E. Kim,[27] M. J. Kim,[17] S. B. Kim,[27] S. H. Kim,[54] Y. K. Kim,[13] N. Kimura,[54] L. Kirsch,[6] S. Klimenko,[18] M. Klute,[32] B. Knuteson,[32] B. R. Ko,[16] S. A. Koay,[10] K. Kondo,[56] D. J. Kong,[27] J. Konigsberg,[18] A. Korytov,[18] A. V. Kotwal,[16] J. Kraus,[24] M. Kreps,[26] J. Kroll,[44] N. Krumnack,[4] M. Kruse,[16] V. Krutelyov,[10] T. Kubo,[54] S. E. Kuhlmann,[2] T. Kuhr,[26] N. P. Kulkarni,[57] Y. Kusakabe,[56] S. Kwang,[13] A. T. Laasanen,[47] S. Lai,[33] S. Lami,[45] S. Lammel,[17] M. Lancaster,[30] R. L. Lander,[7] K. Lannon,[38] A. Lath,[51] G. Latino,[45] I. Lazzizzera,[42] T. LeCompte,[2] J. Lee,[48] J. Lee,[27] Y. J. Lee,[27] S. W. Lee,[52,r] R. Lefèvre,[20] N. Leonardo,[32] S. Leone,[45] S. Levy,[13] J. D. Lewis,[17] C. Lin,[59] C. S. Lin,[28] J. Linacre,[41] M. Lindgren,[17] E. Lipeles,[9] A. Lister,[7] D. O. Litvintsev,[17] T. Liu,[17] N. S. Lockyer,[44] A. Loginov,[59] M. Loreti,[42] L. Lovas,[14] R.-S. Lu,[1] D. Lucchesi,[42] J. Lueck,[26] C. Luci,[50] P. Lujan,[28] P. Lukens,[17] G. Lungu,[18] L. Lyons,[41] J. Lys,[28] R. Lysak,[14] E. Lytken,[47] P. Mack,[26] D. MacQueen,[33] R. Madrak,[17] K. Maeshima,[17] K. Makhoul,[32] T. Maki,[23] P. Maksimovic,[25] S. Malde,[41] S. Malik,[30] G. Manca,[29] A. Manousakis,[15,b] F. Margaroli,[47] C. Marino,[26] C. P. Marino,[24] A. Martin,[59] M. Martin,[25] V. Martin,[21,k] M. Martínez,[3] R. Martínez-Ballarín,[31] T. Maruyama,[54] P. Mastrandrea,[50] T. Masubuchi,[54] M. E. Mattson,[57] P. Mazzanti,[5] K. S. McFarland,[48] P. McIntyre,[52] R. McNulty,[29,j] A. Mehta,[29] P. Mehtala,[23] S. Menzemer,[11,l] A. Menzione,[45] P. Merkel,[47] C. Mesropian,[49] A. Messina,[35] T. Miao,[17] N. Miladinovic,[6] J. Miles,[32] R. Miller,[35] C. Mills,[22] M. Milnik,[26] A. Mitra,[1] G. Mitselmakher,[18] H. Miyake,[54] S. Moed,[22] N. Moggi,[5] C. S. Moon,[27] R. Moore,[17] M. Morello,[45] P. Movilla Fernandez,[28] J. Mülmenstädt,[28] A. Mukherjee,[17] Th. Muller,[26] R. Mumford,[25] P. Murat,[17] M. Mussini,[5] J. Nachtman,[17] Y. Nagai,[54] A. Nagano,[54] J. Naganoma,[56] K. Nakamura,[54]

I. Nakano,[39] A. Napier,[55] V. Necula,[16] C. Neu,[44] M. S. Neubauer,[24] J. Nielsen,[28,g] L. Nodulman,[2] M. Norman,[9] O. Norniella,[24] E. Nurse,[30] S. H. Oh,[16] Y. D. Oh,[27] I. Oksuzian,[18] T. Okusawa,[40] R. Oldeman,[29] R. Orava,[23] K. Osterberg,[23] S. Pagan Griso,[42] C. Pagliarone,[45] E. Palencia,[17] V. Papadimitriou,[17] A. Papaikonomou,[26] A. A. Paramonov,[13] B. Parks,[38] S. Pashapour,[33] J. Patrick,[17] G. Pauletta,[53] M. Paulini,[12] C. Paus,[32] D. E. Pellett,[7] A. Penzo,[53] T. J. Phillips,[16] G. Piacentino,[45] J. Piedra,[43] L. Pinera,[18] K. Pitts,[24] C. Plager,[8] L. Pondrom,[58] X. Portell,[3] O. Poukhov,[15] N. Pounder,[41] F. Prakoshyn,[15] A. Pronko,[17] J. Proudfoot,[2] F. Ptohos,[17,i] G. Punzi,[45] J. Pursley,[58] J. Rademacker,[41,d] A. Rahaman,[46] V. Ramakrishnan,[58] N. Ranjan,[47] I. Redondo,[31] B. Reisert,[17] V. Rekovic,[36] P. Renton,[41] M. Rescigno,[50] S. Richter,[26] F. Rimondi,[5] L. Ristori,[45] A. Robson,[21] T. Rodrigo,[11] E. Rogers,[24] S. Rolli,[55] R. Roser,[17] M. Rossi,[53] R. Rossin,[10] P. Roy,[33] A. Ruiz,[11] J. Russ,[12] V. Rusu,[17] H. Saarikko,[23] A. Safonov,[52] W. K. Sakumoto,[48] G. Salamanna,[50] O. Saltó,[3] L. Santi,[53] S. Sarkar,[50] L. Sartori,[45] K. Sato,[17] A. Savoy-Navarro,[43] T. Scheidle,[26] P. Schlabach,[17] E. E. Schmidt,[17] M. A. Schmidt,[13] M. P. Schmidt,[59] M. Schmitt,[37] T. Schwarz,[7] L. Scodellaro,[11] A. L. Scott,[10] A. Scribano,[45] F. Scuri,[45] A. Sedov,[47] S. Seidel,[36] Y. Seiya,[40] A. Semenov,[15] L. Sexton-Kennedy,[17] A. Sfyria,[20] S. Z. Shalhout,[57] M. D. Shapiro,[28] T. Shears,[29] P. F. Shepard,[46] D. Sherman,[22] M. Shimojima,[54,o] M. Shochet,[13] Y. Shon,[58] I. Shreyber,[20] A. Sidoti,[45] P. Sinervo,[33] A. Sisakyan,[15] A. J. Slaughter,[17] J. Slaunwhite,[38] K. Sliwa,[55] J. R. Smith,[7] F. D. Snider,[17] R. Snihur,[33] M. Soderberg,[34] A. Soha,[7] S. Somalwar,[51] V. Sorin,[35] J. Spalding,[17] F. Spinella,[45] T. Spreitzer,[33] P. Squillacioti,[45] M. Stanitzki,[59] R. St. Denis,[21] B. Stelzer,[8] O. Stelzer-Chilton,[41] D. Stentz,[37] J. Strologas,[36] D. Stuart,[10] J. S. Suh,[27] A. Sukhanov,[18] H. Sun,[55] I. Suslov,[15] T. Suzuki,[54] A. Taffard,[24,f] R. Takashima,[39] Y. Takeuchi,[54] R. Tanaka,[39] M. Tecchio,[34] P. K. Teng,[1] K. Terashi,[49] J. Thom,[17,h] A. S. Thompson,[21] G. A. Thompson,[24] E. Thomson,[44] P. Tipton,[59] V. Tiwari,[12] S. Tkaczyk,[17] D. Toback,[52] S. Tokar,[14] K. Tollefson,[35] T. Tomura,[54] D. Tonelli,[17] S. Torre,[19] D. Torretta,[17] S. Tourneur,[43] W. Trischuk,[33] Y. Tu,[44] N. Turini,[45] F. Ukegawa,[54] S. Uozumi,[54] S. Vallecorsa,[20] N. van Remortel,[23] A. Varganov,[34] E. Vataga,[36] F. Vázquez,[18,m] G. Velev,[17] C. Vellidis,[45,b] V. Veszpremi,[47] M. Vidal,[31] R. Vidal,[17] I. Vila,[11] R. Vilar,[11] T. Vine,[30] M. Vogel,[36] I. Volobouev,[28,r] G. Volpi,[45] F. Würthwein,[9] P. Wagner,[44] R. G. Wagner,[2] R. L. Wagner,[17] J. Wagner-Kuhr,[26] W. Wagner,[26] T. Wakisaka,[40] R. Wallny,[8] S. M. Wang,[1] A. Warburton,[33] D. Waters,[30] M. Weinberger,[52] W. C. Wester III,[17] B. Whitehouse,[55] D. Whiteson,[44,f] A. B. Wicklund,[2] E. Wicklund,[17] G. Williams,[33] H. H. Williams,[44] P. Wilson,[17] B. L. Winer,[38] P. Wittich,[17,h] S. Wolbers,[17] C. Wolfe,[13] T. Wright,[34] X. Wu,[20] S. M. Wynne,[29] A. Yagil,[9] K. Yamamoto,[40] J. Yamaoka,[51] T. Yamashita,[39] C. Yang,[59] U. K. Yang,[13,n] Y. C. Yang,[27] W. M. Yao,[28] G. P. Yeh,[17] J. Yoh,[17] K. Yorita,[13] T. Yoshida,[40] G. B. Yu,[48] I. Yu,[27] S. S. Yu,[17] J. C. Yun,[17] L. Zanello,[50] A. Zanetti,[53] I. Zaw,[22] X. Zhang,[24] Y. Zheng,[8,c] and S. Zucchelli[5]

(CDF Collaboration)[a]

[1]*Institute of Physics, Academia Sinica, Taipei, Taiwan 11529, People's Republic of China*
[2]*Argonne National Laboratory, Argonne, Illinois 60439, USA*
[3]*Institut de Fisica d'Altes Energies, Universitat Autonoma de Barcelona, E-08193, Bellaterra (Barcelona), Spain*
[4]*Baylor University, Waco, Texas 76798, USA*
[5]*Istituto Nazionale di Fisica Nucleare, University of Bologna, I-40127 Bologna, Italy*
[6]*Brandeis University, Waltham, Massachusetts 02254, USA*
[7]*University of California, Davis, Davis, California 95616, USA*
[8]*University of California, Los Angeles, Los Angeles, California 90024, USA*
[9]*University of California, San Diego, La Jolla, California 92093, USA*
[10]*University of California, Santa Barbara, Santa Barbara, California 93106, USA*
[11]*Instituto de Fisica de Cantabria, CSIC-University of Cantabria, 39005 Santander, Spain*
[12]*Carnegie Mellon University, Pittsburgh, Pennsylvania 15213, USA*
[13]*Enrico Fermi Institute, University of Chicago, Chicago, Illinois 60637, USA*
[14]*Comenius University, 842 48 Bratislava, Slovakia and Institute of Experimental Physics, 040 01 Kosice, Slovakia*
[15]*Joint Institute for Nuclear Research, RU-141980 Dubna, Russia*
[16]*Duke University, Durham, North Carolina 27708, USA*
[17]*Fermi National Accelerator Laboratory, Batavia, Illinois 60510, USA*
[18]*University of Florida, Gainesville, Florida 32611, USA*
[19]*Laboratori Nazionali di Frascati, Istituto Nazionale di Fisica Nucleare, I-00044 Frascati, Italy*
[20]*University of Geneva, CH-1211 Geneva 4, Switzerland*
[21]*Glasgow University, Glasgow G12 8QQ, United Kingdom*
[22]*Harvard University, Cambridge, Massachusetts 02138, USA*
[23]*Division of High Energy Physics, Department of Physics, University of Helsinki and Helsinki Institute of Physics, FIN-00014, Helsinki, Finland*

[24]*University of Illinois, Urbana, Illinois 61801, USA*
[25]*The Johns Hopkins University, Baltimore, Maryland 21218, USA*
[26]*Institut für Experimentelle Kernphysik, Universität Karlsruhe, 76128 Karlsruhe, Germany*
[27]*Center for High Energy Physics: Kyungpook National University, Daegu 702-701, Korea;*
Seoul National University, Seoul 151-742, Korea;
Sungkyunkwan University, Suwon 440-746, Korea;
Korea Institute of Science and Technology Information, Daejeon, 305-806, Korea;
Chonnam National University, Gwangju, 500-757, Korea
[28]*Ernest Orlando Lawrence Berkeley National Laboratory, Berkeley, California 94720, USA*
[29]*University of Liverpool, Liverpool L69 7ZE, United Kingdom*
[30]*University College London, London WC1E 6BT, United Kingdom*
[31]*Centro de Investigaciones Energeticas Medioambientales y Tecnologicas, E-28040 Madrid, Spain*
[32]*Massachusetts Institute of Technology, Cambridge, Massachusetts 02139, USA*
[33]*Institute of Particle Physics: McGill University, Montréal, Canada H3A 2T8;*
and University of Toronto, Toronto, Canada M5S 1A7
[34]*University of Michigan, Ann Arbor, Michigan 48109, USA*
[35]*Michigan State University, East Lansing, Michigan 48824, USA*
[36]*University of New Mexico, Albuquerque, New Mexico 87131, USA*
[37]*Northwestern University, Evanston, Illinois 60208, USA*
[38]*The Ohio State University, Columbus, Ohio 43210, USA*
[39]*Okayama University, Okayama 700-8530, Japan*
[40]*Osaka City University, Osaka 588, Japan*
[41]*University of Oxford, Oxford OX1 3RH, United Kingdom*
[42]*Istituto Nazionale di Fisica Nucleare, University of Padova, Sezione di Padova-Trento, I-35131 Padova, Italy*
[43]*LPNHE, Universite Pierre et Marie Curie/IN2P3-CNRS, UMR7585, Paris, F-75252 France*
[44]*University of Pennsylvania, Philadelphia, Pennsylvania 19104, USA*
[45]*Istituto Nazionale di Fisica Nucleare Pisa, University of Pisa, University of Siena, and Scuola Normale Superiore, I-56127 Pisa, Italy*
[46]*University of Pittsburgh, Pittsburgh, Pennsylvania 15260, USA*
[47]*Purdue University, West Lafayette, Indiana 47907, USA*
[48]*University of Rochester, Rochester, New York 14627, USA*
[49]*The Rockefeller University, New York, New York 10021, USA*
[50]*Istituto Nazionale di Fisica Nucleare, Sezione di Roma 1, University of Rome "La Sapienza," I-00185 Roma, Italy*
[51]*Rutgers University, Piscataway, New Jersey 08855, USA*
[52]*Texas A&M University, College Station, Texas 77843, USA*
[53]*Istituto Nazionale di Fisica Nucleare, University of Trieste/Udine, Italy*
[54]*University of Tsukuba, Tsukuba, Ibaraki 305, Japan*
[55]*Tufts University, Medford, Massachusetts 02155, USA*
[56]*Waseda University, Tokyo 169, Japan*
[57]*Wayne State University, Detroit, Michigan 48201, USA*
[58]*University of Wisconsin, Madison, Wisconsin 53706, USA*
[59]*Yale University, New Haven, Connecticut 06520, USA*

(Received 25 July 2007; published 16 January 2008)

We report the observation of the exclusive decay $B_s^0 \to D_s^- D_s^+$ at the 7.5 standard deviation level using 355 pb^{-1} of data collected by the CDF II detector in $p\bar{p}$ collisions at $\sqrt{s} = 1.96$ TeV at the Fermilab Tevatron. We measure the relative branching ratio $\mathcal{B}(B_s^0 \to D_s^- D_s^+)/\mathcal{B}(B^0 \to D^- D_s^+) = 1.44^{+0.48}_{-0.44}$. Using the world average value for $\mathcal{B}(B^0 \to D^- D_s^+)$, we find $\mathcal{B}(B_s^0 \to D_s^- D_s^+) = (9.4^{+4.4}_{-4.2}) \times 10^{-3}$. This provides a lower bound $\Delta\Gamma_s^{CP}/\Gamma_s \geq 2\mathcal{B}(B_s^0 \to D_s^- D_s^+) > 1.2 \times 10^{-2}$ at 95% C.L.

DOI: 10.1103/PhysRevLett.100.021803 PACS numbers: 13.25.Hw, 14.40.Nd

The $B_s^0 - \bar{B}_s^0$ system exhibits mixing, with two distinct mass eigenstates B_H and B_L having a mass difference $\Delta m_s = m_s^H - m_s^L$, which has recently been measured [1]. In the standard model, these two states have decay widths Γ_s^L and Γ_s^H, with difference $\Delta\Gamma_s = \Gamma_s^L - \Gamma_s^H$ and average $\Gamma_s = (\Gamma_s^L + \Gamma_s^H)/2$. To good approximation, the two mass eigenstates are expected to be eigenstates of CP: B_s^{even} and B_s^{odd}, so that $\Delta\Gamma_s \approx \Delta\Gamma_s^{CP}$, where $\Delta\Gamma_s^{CP} = \Gamma(B_s^{\mathrm{even}}) - \Gamma(B_s^{\mathrm{odd}})$. The Standard Model predicts $\Delta\Gamma_s/\Gamma_s = 0.147 \pm 0.060$ [2] with a reasonably small uncertainty. A measurement of this quantity can therefore provide a sensitive test and in case of a discrepancy it would be a good indicator for new physics. Measuring the B_s^0 decay rate to $D_s^{(*)-} D_s^{(*)+}$, where $D_s^{(*)\pm}$ stands for either $D_s^\pm$ or $D_s^{*\pm}$, determines $\Delta\Gamma_s^{CP}/\Gamma_s$, assuming the $b \to c\bar{c}s$ transitions are dominated by these decays, and neglecting small

CP-odd components [3]:

$$\frac{\Delta\Gamma_s^{CP}}{\Gamma_s} = 2\mathcal{B}(B_s^0 \to D_s^{(*)-} D_s^{(*)+}). \tag{1}$$

The inclusive measurement of the $B_s^0 \to D_s^{(*)-} D_s^{(*)+}$ decay rate has been reported previously [4] using $B_s^0 \to \phi\phi X$ correlations. In this Letter we present the first observation of the exclusive decay $B_s^0 \to D_s^- D_s^+$ [5], measure the ratio of its branching fraction with respect to that for $B^0 \to D^- D_s^+$, and set a lower bound on $\Delta\Gamma_s^{CP}/\Gamma_s$. We use CDF II detector data corresponding to 355 pb^{-1} of integrated luminosity of $p\bar{p}$ collisions at $\sqrt{s} = 1.96$ TeV at the Fermilab Tevatron [6].

This analysis depends primarily on the charged particle tracking systems. Charged particle tracks are reconstructed using the hits in the silicon microstrip detector system and the central outer tracker (COT) in the pseudorapidity range $|\eta| \leq 1.0$, where η is defined as $-\ln\tan(\theta/2)$ and θ represents the angle between the particle and the proton beam direction [7]. Both detectors are inside a 1.4 T uniform magnetic field. The silicon detector is composed of L00 (single layer of silicon microstrip sensors close to the beam pipe), the silicon vertex detector (SVX II) (five cylindrical layers of double-sided sensors), and intermediate silicon layers, providing up to 8 coordinate measurements in the r-ϕ view [8]. Surrounding the SVX is the COT, a cylindrical drift chamber with 96 layers of sense wires [9].

A sample rich in charm and beauty hadrons is selected by a three-level displaced track trigger. At level 1, tracks are reconstructed in the COT by the track trigger processor (Extremely Fast Tracker, XFT) [10]. The trigger requires two tracks with transverse momenta $p_T > 2$ GeV$/c$ and the scalar sum $p_{T1} + p_{T2} > 4.0$ GeV$/c$. The level 2 silicon vertex trigger [11] associates SVX II r-ϕ position measurements with Extremely Fast Tracker tracks and provides a precise measurement of the track impact parameter (d_0), the distance of closest approach of the track helix to the beam axis in the transverse plane. Decays of heavy flavor particles are identified by requiring two tracks with 0.12 mm $\leq d_0 \leq$ 1 mm and an opening angle in the transverse plane $2° \leq |\Delta\phi| \leq 90°$. A requirement $L_{xy} >$ 0.2 mm is also applied, where L_{xy} is defined as the distance in the transverse plane from the beam line to the two-track vertex projected onto the two-track momentum vector. The level 3 trigger applies the level 1 and level 2 selection requirements after a full event reconstruction.

We measure the branching fraction ratio $\mathcal{B}(B_s^0 \to D_s^- D_s^+)/\mathcal{B}(B^0 \to D^- D_s^+)$ in which the D_s^+ meson decay rates and part of the systematic uncertainties cancel. In searching for $B_s^0 \to D_s^- D_s^+$ we require the decay $D_s^- \to \phi\pi^-$. To enhance the search sensitivity we reconstruct D_s^+ meson candidates in the $\phi\pi^+$, $\bar{K}^{*0}K^+$, or $\pi^+\pi^+\pi^-$ decay channels for both the B^0 and B_s^0 signals. The ratio is measured independently for three D_s^+ decay modes and is calculated using

$$\frac{\mathcal{B}(B_s^0 \to D_s^- D_s^+)}{\mathcal{B}(B^0 \to D^- D_s^+)} = \frac{N_{B_s^0}}{N_{B^0}} \frac{\epsilon_{B^0}}{\epsilon_{B_s^0}} \frac{f_d}{f_s} \frac{\mathcal{B}(D^- \to K^+\pi^-\pi^-)}{\mathcal{B}(D_s^- \to \phi\pi^-)}, \tag{2}$$

where $N_{B_s^0}$ and N_{B^0} are the measured signal yields, $\epsilon_{B^0}/\epsilon_{B_s^0}$ is the ratio of reconstruction and trigger efficiencies extracted from Monte Carlo simulation, f_s/f_d is the ratio of b quark fragmentation fractions into B_s^0 and B^0 mesons, and $\mathcal{B}(D^- \to K^+\pi^-\pi^-)/\mathcal{B}(D_s^- \to \phi\pi^-)$ is the ratio of branching fractions determined by other experiments.

All tracks used in reconstruction must have $p_T >$ 350 MeV$/c$ and are assumed to be either pions or kaons depending on the specific reconstruction hypothesis. The reconstruction of $B^0 \to D^-(K^+\pi^-\pi^-)D_s^+(\phi\pi^+)$, for example, begins by searching for $D_s^+ \to \phi\pi^+$ candidates. We require two oppositely charged tracks to form $\phi \to K^+K^-$ and then add a third track to form $D_s^+ \to \phi\pi^+$. The reconstruction of D^- mesons uses the $D^- \to K^+\pi^-\pi^-$ mode. We reconstruct $B^0 \to D^- D_s^+$ candidates by applying a fit to six tracks with constraints on a primary B meson decay vertex, two secondary D meson decay vertices, and the masses of the D mesons.

Monte Carlo simulations are used to optimize the selection requirements, to derive fitting functions for signal and background, and to determine the trigger and reconstruction efficiencies. Single B hadrons are generated without fragmentation products of underlying event particles, and their decays are simulated using EVTGEN [12]. The detector response, including the trigger, is modeled using the CDF simulation package [13]. The selection requirements are optimized by maximizing the significance of the Monte Carlo simulated signal, scaled to the expected yield, relative to the combinatorial background using a method valid for low statistics [14]. Combinatorial background is fitted in the interval $[5.4, 6.0]$ GeV$/c^2$ and extrapolated into a 60 MeV$/c^2$ wide signal region centered around the appropriate B meson mass. Selection requirements are made on the minimum p_T of the tracks, the impact parameter of the B meson, and the χ^2 masses of ϕ and K^{*0} candidates. We also make requirements on the significance of the L_{xy} measurement, $L_{xy}/\sigma(L_{xy})$, where $\sigma(L_{xy})$ is the L_{xy} uncertainty, of B and D meson vertices, and of the displacement of the D meson vertices with respect to the B meson vertex. For decays involving resonant states, we require 1010 MeV$/c^2 < m(K^+K^-) <$ 1029 MeV$/c^2$ for ϕ candidates and 840 MeV$/c^2 < m(K^-\pi^+) <$ 940 MeV$/c^2$ for K^{*0} candidates. The background from $\bar{B}^0 \to D^+(K^-\pi^+\pi^+)D_s^-(\phi\pi^-)$ is removed from the $B_s^0 \to D_s^-(\phi\pi^-)D_s^+(\bar{K}^{*0}K^+)$ signal by reconstructing $D_s^+ \to \bar{K}^{*0}K^+$ as $D^+ \to K^-\pi^+\pi^+$ and removing events with the D^+ candidate mass in the range 1845 MeV$/c^2 <$ $m(K^-\pi + \pi^+) <$ 1893 MeV$/c^2$.

Figure 1 shows the reconstructed mass spectra for $B_s^0 \to D_s^- D_s^+$ and $B^0 \to D^- D_s^+$ decays. The signal yields $N_{B_s^0}$ and N_{B^0} are extracted from a binned likelihood fit of these

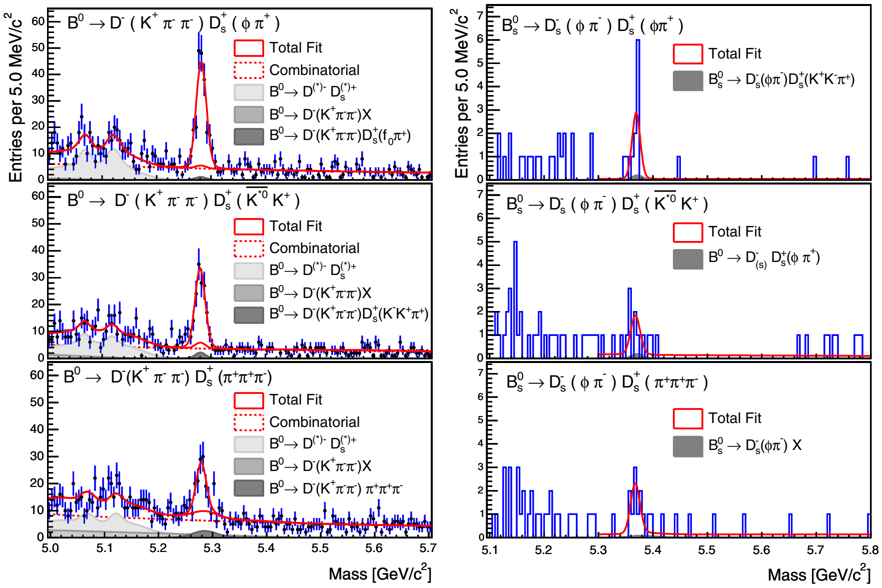

FIG. 1 (color online). Mass spectra for $B^0 \to D^- D_s^+$ (left) and $B_s^0 \to D_s^- D_s^+$ (right) where $D_s^+ \to \phi\pi^+$ (top), $D_s^+ \to \bar{K}^{*0}K^+$ (middle), $D_s^+ \to \pi^+\pi^+\pi^-$ (bottom). The decomposition of the background into combinatorial background and several backgrounds from B hadron decays is shown. For B^0 decays data are represented with dots and error bars, while for the small event yield B_s^0 channels a histogram is shown.

spectra. The fitting functions for all the modes have terms describing the signal, combinatorial background, partially reconstructed B hadrons, and contributions from B decays to different D_s^+ decay modes. The combinatorial background is represented by the sum of a constant plus an exponential. The signal and partially reconstructed modes are fitted with templates that have fixed shapes derived from simulation and floating normalizations. Each signal template is parametrized by two Gaussians with different widths and a common mean.

In fitting $B_s^0 \to D_s^- D_s^+$ distributions, we fix the signal masses to Particle Data Group values [15], and we fix the Gaussian signal widths, dominated by detector resolution, to the values obtained from Monte Carlo simulation. We also limit the mass range in the fit to value above 5.3 GeV$/c^2$ avoiding a detailed description of the well separated physics background.

We treat the background from the decay mode $B^0 \to D^-\pi^+\pi^+\pi^-$ to the signal for $B^0 \to D^-(K^+\pi^-\pi^-)\times D_s^+(\bar{K}^{*0}K^+)$ and $B^0 \to D^-(K^+\pi^-\pi^-)D_s^+(\pi^+\pi^+\pi^-)$ modes by introducing templates normalized to the B^0 yield. Similarly, we introduce the template normalized to the B_s^0 yield to model $B_s^0 \to D_s^-(\phi\pi^-)\pi^+\pi^+\pi^-$ background under the signal for $B_s^0 \to D_s^-(\phi\pi^-)\times D_s^+(\pi^+\pi^+\pi^-)$ mode. These corrections lead to a less than 2% change in the signal.

Monte Carlo studies show that a B meson signal, reconstructed in a specific D_s^+ decay mode, have contributions from misreconstructed B meson candidates decaying through other D_s channels. The decay $B^0 \to D^- D_s^+$, followed by $D_s^+ \to f_0(980)(K^+K^-)\pi^+$, contributes to the reconstructed $B^0 \to D^-(K^+\pi^-\pi^-)D_s^+(\phi\pi^+)$. Similarly, B meson decays followed by a nonresonant $D_s^+ \to K^+K^-\pi^+$ contribute to the B meson signal reconstructed with $D_s^+ \to \bar{K}^{*0}K^+$. The $D_s^+ \to K^+K^-\pi^+$ decay model takes into account the measured branching fractions of its resonant substructure [16]. The aforementioned effects are taken into account by introducing correction templates

TABLE I. Summary of event yields, efficiencies, measured ratios of branching fractions, and corresponding uncertainties for three D_s^+ decay modes.

	$\phi\pi^+$	$\bar{K}^{*0}K^+$	$\pi^+\pi^+\pi^-$
$N(B^0 \to D^- D_s^+)$	183 ± 15	128 ± 13	84 ± 13
$N(B_s^0 \to D_s^- D_s^+)$	$9.2^{+3.5}_{-2.9}$	$6.0^{+3.4}_{-2.7}$	$8.3^{+3.5}_{-2.8}$
$\epsilon(B_s^0 \to D_s^- D_s^+)/\epsilon(B^0 \to D^- D_s^+)$	0.88 ± 0.03	0.53 ± 0.02	0.63 ± 0.02
$\mathcal{B}(B_s^0 \to D_s^- D_s^+)/\mathcal{B}(B^0 \to D^- D_s^+)$	$0.98^{+0.38}_{-0.32}$	$1.51^{+0.87}_{-0.70}$	$2.67^{+1.20}_{-0.99}$
systematic uncertainty	$+0.06/-0.08$	$+0.15/-0.25$	$+0.27/-0.29$
(f_s/f_d) uncertainty	± 0.14	± 0.22	± 0.39
$\mathcal{B}(D_s^- \to \phi\pi^-)/\mathcal{B}(D^- \to K^+\pi^-\pi^-)$ uncertainty	± 0.13	± 0.20	± 0.36

TABLE II. Systematic uncertainties in [%] for the B_s^0/B^0 relative branching fraction measurements for three D_s^+ decay modes.

	$\phi\pi^+$	$\bar{K}^{*0}K^+$	$\pi^+\pi^+\pi^-$
$B^0 \to D^- D_s^+$ fit	± 2.3	± 4.2	± 8.4
$B_s^0 \to D_s^- D_s^+$ fit	± 4.4	± 8.2	± 4.6
B meson p_T spectrum	± 3.0	± 3.0	± 3.0
B_s^0 lifetime	± 2.0	± 2.0	± 2.0
trigger	± 1.0	± 1.0	± 1.0
$D_s^+ \to \pi^+\pi^+\pi^-$ composition	-	-	± 3.0
optimization bias	-5.0	-13.0	-4.0
Total	${}^{+6.2}_{-8.0}$	${}^{+9.9}_{-16.4}$	${}^{+10.3}_{-11.0}$

with relative normalizations derived from Monte Carlo simulations and result in a 4% correction to the signal yield. Other b hadron backgrounds are described with templates derived from semigeneric simulations ($B \to D_{(s)}^- X$), where one of the $D_{(s)}^-$ mesons is forced to decay in the signal channel and the rest of the decay chain (X) follows the best available measurement of branching fractions.

Yields and ratios of reconstruction efficiencies extracted from signal simulations are summarized in Table I. Using Eq. (2) and the latest PDG [15] values $f_s/f_d = 0.259 \pm 0.038$, and $\mathcal{B}(D_s^- \to \phi\pi^-) \times \mathcal{B}(\phi \to K^+K^-) = (2.16 \pm 0.28) \times 10^{-2}$, we calculate the ratio of branching fractions $\mathcal{B}(B_s^0 \to D_s^- D_s^+)/\mathcal{B}(B^0 \to D^- D_s^+)$ for the three D_s^+ modes shown in Table I along with corresponding statistical uncertainties, systematic uncertainties discussed below, and the uncertainties from the measurements of f_s/f_d and $\mathcal{B}(D_s^- \to \phi\pi^-)/\mathcal{B}(D^- \to K^+\pi^-\pi^-)$.

The systematic uncertainties, summarized in Table II, are evaluated from the change in the ratio of the branching fractions $\mathcal{B}(B_s^0 \to D_s^- D_s^+)/\mathcal{B}(B^0 \to D^- D_s^+)$ for each effect under consideration. Fit systematic uncertainties are estimated by varying the fit window, binning, and template parameters. The normalizations of background templates underneath the signal peaks are varied using the measured branching fractions [15] within their uncertainties and the effect is included in the fit systematics in Table II. The uncertainty due to the B meson p_T spectrum is evaluated by comparing the efficiency determined from simulation based on next-to-leading-order calculations [17] and on the measured B hadron spectrum [18]. The effect of meson lifetimes is studied by varying the world average B_s^0 and B^0 lifetimes within their uncertainties in the simulations. Trigger-related systematic uncertainties are estimated from simulations. The effects due to the limited knowledge of the $D_s^+ \to \pi^+\pi^+\pi^-$ composition are studied by varying the relative branching fractions of the components of the decay within their PDG [15] uncertainties. Finally, using the combinatorial background from data to optimize the selection introduces a bias. This effect has been estimated using simulation based on the expected combinatorial background distribution.

The significance of the $B_s^0 \to D_s^- D_s^+$ signal is given by the ratio of likelihoods of the mass fits, where we use the one of full fit model divided by the one of the same model but excluding the signal component. The individual significances of the signal reconstructed with $B_s^0 \to D_s^-(\phi\pi^-)D_s^+(\phi\pi^+)$, $B_s^0 \to D_s^-(\phi\pi^-)D_s^+(\bar{K}^{*0}K^+)$, and $B_s^0 \to D_s^-(\phi\pi^-)D_s^+(\pi^+\pi^+\pi^-)$ decay modes are 5.8σ, 3.4σ, and 4.4σ, respectively. From the product of three likelihoods we find the combined result consistent with an observation of $B_s^0 \to D_s^- D_s^+$ at a 7.5σ significance.

When combining the three results, the fit systematic uncertainties are weighed by the measured yields. The rest of the systematic uncertainties, except for the $D_s^+ \to \pi^+\pi^+\pi^-$ composition uncertainty, are considered common for all three modes. We find

$$\frac{\mathcal{B}(B_s^0 \to D_s^- D_s^+)}{\mathcal{B}(B^0 \to D^- D_s^+)} = 1.44^{+0.38}_{-0.31}(\text{stat})^{+0.08}_{-0.12}(\text{syst}) \pm 0.21(f_s/f_d) \pm 0.20\left(\frac{\mathcal{B}(D^- \to K^+\pi^-\pi^-)}{\mathcal{B}(D_s^- \to \phi\pi^-)}\right), \quad (3)$$

which we combine with $\mathcal{B}(B^0 \to D^- D_s^+) = (6.5 \pm 2.1) \times 10^{-3}$ [15] and determine

$$\mathcal{B}(B_s^0 \to D_s^- D_s^+) = (9.4^{+4.4}_{-4.2}) \times 10^{-3}, \quad (4)$$

from which we derive a lower limit on $\Delta\Gamma_s^{CP}/\Gamma$:

$$\frac{\Delta\Gamma_s^{CP}}{\Gamma_s} = 2\mathcal{B}(B_s^0 \to D_s^{(*)-} D_s^{(*)+}) \geq 2\mathcal{B}(B_s^0 \to D_s^- D_s^+) \geq 1.2 \times 10^{-2} \quad \text{at} \quad 95\%\,\text{C.L.} \quad (5)$$

In the derivation of the lower limit we take into account the Poisson statistical fluctuations of the signal yields and the Gaussian distribution for systematics uncertainties.

We have presented the first observation of the decay $B_s^0 \to D_s^- D_s^+$ and have measured its branching fraction with respect to $B^0 \to D^- D_s^+$. We set a lower bound on $\Delta\Gamma_s^{CP}/\Gamma_s$, which at the 95% confidence level requires a nonzero decay rate difference and agrees with theoretical predictions [2] and other experimental data: $-0.06 < \Delta\Gamma_s/\Gamma_s < 0.28$ at the 95% confidence level [15].

We thank the Fermilab staff and the technical staffs of the participating institutions for their vital contributions. This work was supported by the U.S. Department of Energy and National Science Foundation; the Italian Istituto Nazionale di Fisica Nucleare; the Ministry of Education, Culture, Sports, Science, and Technology of Japan; the Natural Sciences and Engineering Research Council of Canada; the National Science Council of the Republic of China; the Swiss National Science Foundation; the A. P. Sloan Foundation; the Bundesministerium für Bildung und Forschung, Germany; the Korean Science and Engineering Foundation and the Korean Research Foundation; the Particle Physics and Astronomy Research Council and the Royal Society, United Kingdom; the Russian Foundation for Basic Research; the Comisión Interministerial de Ciencia y Tecnología, Spain; in part by the European Community's Human Potential Programme under Contract No. HPRN-CT-2002-00292; and the Academy of Finland.

[a]Visiting scientists from
[b]University of Athens, 15784 Athens, Greece.
[c]Chinese Academy of Sciences, Beijing 100864, China.
[d]University of Bristol, Bristol BS8 1TL, United Kingdom.
[e]University Libre de Bruxelles, B-1050 Brussels, Belgium.
[f]University of California, Irvine, Irvine, CA 92697, USA.
[g]University of California, Santa Cruz, Santa Cruz, CA 95064, USA.
[h]Cornell University, Ithaca, NY 14853, USA.
[i]University of Cyprus, Nicosia CY-1678, Cyprus.
[j]University College Dublin, Dublin 4, Ireland.
[k]University of Edinburgh, Edinburgh EH9 3JZ, United Kingdom.
[l]University of Heidelberg, D-69120 Heidelberg, Germany.
[m]Universidad Iberoamericana, Mexico D.F., Mexico.
[n]University of Manchester, Manchester M13 9PL, England.
[o]Nagasaki Institute of Applied Science, Nagasaki, Japan.
[p]University de Oviedo, E-33007 Oviedo, Spain.
[q]Queen Mary, University of London, London, E1 4NS, England.
[r]Texas Tech University, Lubbock, TX 79409, USA.
[s]IFIC (CSIC-Universitat de Valencia), 46071 Valencia, Spain.

[1] A. Abulencia *et al.* (CDF Collaboration), Phys. Rev. Lett. **97**, 242003 (2006).
[2] A. Lenz and U. Nierste, J. High Energy Phys. 06 (2007) 072.
[3] I. Dunietz, R. Fleischer, and U. Nierste, Phys. Rev. D **63**, 114015 (2001).
[4] R. Barate *et al.* (ALEPH Collaboration), Phys. Lett. B **486**, 286 (2000).
[5] The charge conjugate state is implied throughout the paper. Our notation is such that, e.g., $B_s^0 \to D_s^-(\phi\pi^-)D_s^+(\phi\pi^+)$ refers to $B_s^0 \to D_s^- D_s^+$, followed by $D_s^- \to \phi\pi^-$ and $D_s^+ \to \phi\pi^+$, followed by $\phi \to K^+K^-$.
[6] D. Acosta *et al.* (CDF Collaboration), Phys. Rev. D **71**, 032001 (2005).
[7] CDF II uses a cylindrical coordinate system in which ϕ is the azimuthal angle, r is the radius from the symmetry axis, y points up, and z points in the proton beam direction with the origin at the center of the detector. The transverse plane is the plane perpendicular to the z axis.
[8] A. Sill *et al.*, Nucl. Instrum. Methods Phys. Res., Sect. A **447**, 1 (2000).
[9] T. Affolder *et al.*, Nucl. Instrum. Methods Phys. Res., Sect. A **526**, 249 (2004).
[10] E. J. Thomson *et al.*, IEEE Trans. Nucl. Sci. **49**, 1063 (2002).
[11] W. Ashmanskas *et al.*, Nucl. Instrum. Methods Phys. Res., Sect. A **518**, 532 (2004).
[12] D. Langle, Nucl. Instrum. Methods Phys. Res., Sect. A **462**, 152 (2001).
[13] E. Gershtein and M. Paulini, arXiv:physics/0306031.
[14] G. Punzi, arXiv:physics/0308063.
[15] W.-M. Yao *et al.*, J. Phys. G **33**, 1 (2006).
[16] Frabetti *et al.* (FNAL E687 Collaboration), Phys. Lett. B **351**, 591 (1995).
[17] P. Nason, S. Dawson, and R. K. Ellis, Nucl. Phys. B **303**, 607 (1988); **327**, 49 (1989).
[18] D. Acosta *et al.* (CDF Collaboration), Phys. Rev. D **71**, 032001 (2005).